Proceedings of the
International Conference on Mechanical Engineering and Renewable Energy 2011
(ICMERE2011) 22- 24 December 2011, Chittagong, Bangladesh

ICMERE2011-PI-107

COMPUTATION OF TURBULENT FLOW OVER A CYLINDER

Md. Taibur Rahman[1], Swachwa Dey[2]

[1] Lecturer, Department of Mechanical and Production Engineering, AUST, Dhaka, Bangladesh.
[2] Project Engineer, Industrial Engineering and Services.

[1]khushbu.cuet@gmail.com, [2]swachwa.dey@hotmail.com

Abstract- *Turbulent flow around cylinder is computed at different flow regimes using finite volume method based on Reynolds-averaged Navier-Stokes (RANS) equations. Two-dimensional flow solver has been used to analyze flow at Reynolds number of 5×10^6. Standard k - epsilon turbulence model are used to capture turbulent flow. Deviation of negative pressure co-efficient from positive pressure co-efficient is smaller for higher velocity in pressure recovery region. The slope of the pressure co-efficient curve is higher for higher diameter of cylinder. Pressure co-efficient is higher negative for larger diameter of cylinder. Skin friction co-efficient increases with the increase of diameter.*

Keywords: Control volume, pressure, velocity, contour, turbulent flow, pressure co-efficient, skin friction, velocity vector, flow regime.

1. INTRODUCTION

Flow over a circular cylinder problem arises in diverse engineering applications such as hydrodynamic loading on marine pipelines, risers, offshore platform support legs, chemical mixing, lift enhancement etc. [1, 2].It is experimentally investigated that when the Reynolds number of flow over a circular cylinder exceeds 48, vortices separate from the boundary layer, and start to move through the downstream, where steady state behavior of the flow turns into a time-dependent state [3]. These periodically moving vortices through the downstream form self-excited oscillations called the von Karman vortex street [2].

Separation from the surface of the cylinder can either be laminar or turbulent according to the regime of the flow in the boundary layer. Flow over a circular cylinder with a Reynolds number between 1,000 and 20,000 is called subcritical since flow separation is entirely laminar, and transition from laminar to turbulent flow happens somewhere at the downstream [4]. Although vortex street is fully turbulent after Re≈20,000, laminar separation sustains at a Reynolds number of 100,000 [5]. Direct Numerical Simulation (DNS), which directly resolves turbulent structures, achieves most accurate computational solutions. However, it requires much finer grids to resolve small structures, and this leads to prohibitive computational costs. On the other hand, Reynolds-Averaged Navier-Stokes Equations (RANS) is an approximation that uses additional equations to model turbulent structures, and to implement its effects to the solution and it requires considerably less computational effort to solve Navier-Stokes equations. Time-dependent problems can be solved by the utilization of Unsteady Reynolds-Averaged Navier-Stokes Equations (URANS). URANS yields satisfactory results for engineering purposes[1]. Additionally, employment of two-dimensional (2D) simulations can reduce computational cost, since the dominant vortex shedding mechanism is effectively two-dimensional [8]. It is also stated in another study [7] that three-dimensionality of the cylinder plays role when length to diameter ratio is smaller than 3.8.

There are several engineering applications that are concerned with the control of the vortices formed behind the cylinder such as vibration control, chemical mixing improvement, dynamic stall control and lift enhancement [2]. Since now, different active control schemes are utilized in literature for damping the vortex-induced oscillations, such as acoustic excitation, rotation of the cylinder, alternate blowing and suction at separation points, and vibration wires in the wake [2].

2. THEORETICAL FORMULATION

CFD is based on the fundamental governing equations of fluid dynamics. The Equations are continuity, momentum, and energy equations. These equations speak physics. They are the mathematical statements of three fundamental physical principles upon which all of fluid dynamics is based:

1. Mass is conserved.
2. Newton's second law, F = ma.
3. Energy is conserved.

2.1 Conservation laws

If we restrict our attention to single-phase fluids, the law of mass conservation expresses the fact that mass cannot

be created in such a fluid system, nor can disappear from it.

At a point on the control surface, the flow velocity is $\vec{v}$, the unit normal vector is $\vec{n}$ and dS denotes an- elemental surface area. For the time rate of change of the total mass inside the finite volume **Ω.** The conserved quantity in this case is the density ρ, surface area $(\vec{v} * \vec{n})$, by convection $\vec{n}$ always points out of the control volume, we speak of Inflow if the product $(\vec{v} * \vec{n})$ is negative, and of outflow if it is positive and hence the mass flow leaves the control volume. Hence integral form of the continuity equation - the conservation law of mass can be represent as:

$$\frac{\partial}{\partial t}\int_{\Omega} \rho d\,\Omega + \oint_{\partial\Omega} \rho(\vec{v} * \vec{n})\, dS = 0 \qquad (2.1)$$

momentum conservation inside an arbitrary control volume R which is fixed in space.

$$\frac{\partial}{\partial t}\int_{\Omega} \rho\vec{v} d\,\Omega + \oint_{\partial\Omega} \rho\vec{v}(\vec{v}\,.\,\vec{n})\, dS =$$

$$\int_{\Omega} \rho\vec{f_e}\, d\Omega - \oint_{\partial\Omega} p\,\vec{n}\mathrm{dS} + \oint_{\partial\Omega} (\bar{\bar{\tau}}\,.\,\vec{n})\,\mathrm{dS} \qquad (2.2)$$

Where, body force per unit volume, denoted as- $\rho\vec{f}_e$, viscous stress tensor as$\bar{\bar{\tau}}$.

The energy equation can be represent as-

$$\frac{\partial}{\partial t}\int_{\Omega} \rho E d\Omega + \oint_{\partial\Omega} \rho H(\vec{v}\,.\,\vec{n})\, dS =$$

$$\int_{\partial\Omega} \kappa(\nabla T\,.\,\vec{n}) dS + \int_{\Omega} (\rho\vec{f_e}\,.\vec{v} + \dot{q_h}) - \oint_{\partial\Omega} p\,(\vec{v}\,.\,\vec{n}\,)\mathrm{dS}$$

$$+ \oint_{\partial\Omega} (\bar{\bar{\tau}}\,.\,\vec{v})\,.\vec{n}\mathrm{dS} \qquad (2.3)$$

We will denote the heat sources - the time rate of heat transfer per unit mass - as $\vec{q}_h$. Together with the rate of work done by the body forces $\vec{f}_e$, total energy E, temperature gradient ∇T.

3. STANDARD K - EPSILON TURBULENCE MODEL

At high Reynolds numbers [11] the rate of dissipation of kinetic energy ϵ is equal to the viscosity multiplied by the fluctuating vorticity. An exact transport equation for the fluctuating vorticity, and thus the dissipation rate, can be derived from the Navier Stokes equation. The k - epsilon model consists of the turbulent kinetic energy equation-

$$\frac{\partial k}{\partial t} + \mathrm{div}\,(\rho\underline{u}k) = \mathrm{div}\left(\left[\mu_{\mathrm{tam}} + \frac{\rho v_t}{\sigma_k}\right]\mathrm{gradk}\right) + \sigma v_t G - \rho\varepsilon \qquad (3.1)$$

And the dissipation rate (ε) equation-

$$\frac{\partial \varepsilon}{\partial t} + \mathrm{div}\,(\rho\underline{u}\varepsilon) = \mathrm{div}\left(\left[\mu_{\mathrm{tam}} + \frac{\rho v_t}{\sigma_\varepsilon}\right]\mathrm{grad}\varepsilon\right) + C_{1\varepsilon}\rho v_t G\frac{\varepsilon}{k} - C_{2\varepsilon}\rho\frac{\varepsilon^2}{k} \qquad (3.2)$$

Where *G* represents the turbulent generation rate – G=2

$$\left(\left[\frac{\partial u}{\partial x}\right]^2 + \left[\frac{\partial v}{\partial y}\right]^2 + \left[\frac{\partial w}{\partial z}\right]^2\right) + \left(\frac{\partial u}{\partial y} + \frac{\partial v}{\partial x}\right)^2 + \left(\frac{\partial u}{\partial z} + \frac{\partial w}{\partial x}\right)^2 + \left(\frac{\partial w}{\partial y} + \frac{\partial v}{\partial z}\right)^2 \qquad (3.3)$$

Model constants are-

$C_{1\varepsilon} = 1.44\,, C_{2\varepsilon} = 1.92\,, C_{\mu} = 0.09, \sigma_k = 1.0\,, \sigma_\varepsilon = 1.3$

4. BOUNDARY CONDITIONS

The bottom and top boundary of the domain is modeled as an axis boundary. Additionally, the left boundary of the domain is modeled as 'velocity inlet', the right boundary is modeled as an 'outflow boundary', and the surface of the body itself is modeled as a 'wall'.

4. METHODOLOGY

For the turbulent CFD simulations, Fluent software is used. Pressure-based Navier-Stokes Equations are solved with double precision and incompressible turbulent flow is modeled in the simulations. Numerical methods and solution algorithms employed in CFD simulations are as follows:

- Pressure-based Navier-Stokes Equations.
- Coupled algorithm for pressure-velocity coupling.
- Second-order upwind method for spatial discretization.
- First-order temporal discretization .
- Least squares cell-based method for calculations of gradients and derivatives.

Operating conditions and fluid properties are selected as density=0.01056 kg/m3, viscosity=1.795x10-5 kg/ms and pressure=872.36 Pa. Free-stream velocity is defined at the inlet boundary with a turbulence intensity of10% and a length scale of 0.07. Outlet-vent boundary condition is applied at the outlet, and top and bottom surfaces are defined as symmetrical. Surface of the cylinder is defined as smooth wall, and no-slip boundary condition is employed. The dimensions of the computational domain are defined as 120 x 40 and the cylinder is placed at the center of this domain. Grid is generated by using quadrilateral elements around the surface of the cylinder, and triangular cells at the rest of the computational domain.

To converge the solution it takes 725 iteration steps shown in fig-1

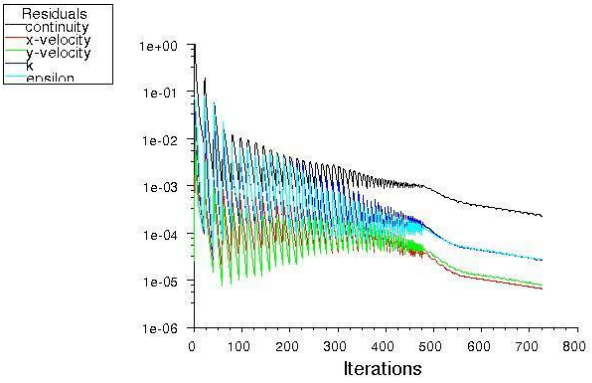

Fig-1: Residuals converging graph.

Table-1: Grid information

Level	Cells	Faces	Nodes	Partitions
0	5636	8579	2943	1

Table-2: Discretization Scheme

Variable	Scheme
Pressure	Standard
Momentum	Second Order Upwind
Turbulence Kinetic Energy	Second Order Upwind
Turbulence Dissipation Rate	Second Order Upwind

Table-3: Solution Limits

Quantity	Limit
Minimum Absolute Pressure	1
Maximum Absolute Pressure	5e+10
Minimum Temperature	1
Minimum Turb. Kinetic Energy	1e-14
Minimum Turb. Dissipation Rate	1e-20
Maximum Turb. Viscosity Ratio	100000

6. RESULTS AND DISCUSSION

Computed results for turbulent flow around cylinder are compared to Achenbach's experimental data [6] for transcitical flow. According to the experimental observation of Achenbach, the flow around a cylinder can be classified into four regions depending on the Reynolds number. In the subcritical region (Re < 3×10^5) the drag coefficient is namely independent of Reynolds number. The critical region (3×10^5 < Re < 4×1065) is characterized by a rapid drop of the drag coefficient. The minimum being reached at the critical Re = 3.7×10^5, with further increase in Reynolds number, C_d slightly increases again which is known as supercritical flow (4×10^5 < Re< 2×10^6) and it seems that the curve is going to reach another maximum. The transition from supercritical to transcritical (Re > 2×10^6) is rather floating. Achenbach's experiment is performed at a transcritical Reynolds number where the flow is considered fully turbulent and thus can be directly compared to the turbulent computational models. In the present study, the turbulent flow is simulated using standard K-EPSILON turbulence model.

Figure-2 shows the flow domain, information about the domain is given in table-1.

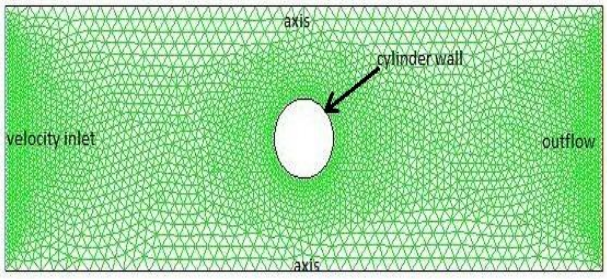

Fig-2: Cylinder grid with boundary condition.

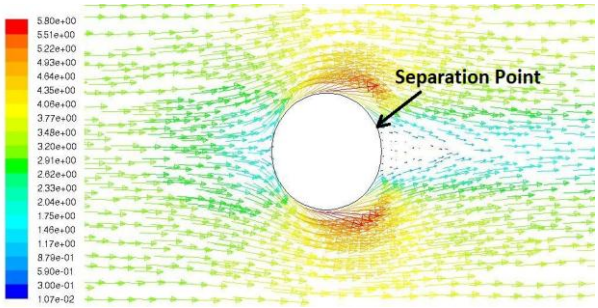

Fig-3: Velocity vector diagram showing separation point.

Figure-3 shows the velocity magnitude at different points of the flow domain. Here different color and size of arrow shows the magnitude of velocity vector. It also shows the characteristics features like stagnation region, flow separation point and the recirculation region. At the point of forward stagnation point and after the flow past the cylinder velocity is less than other place which is shown by blue color. Red color shows the maximum velocity magnitude and yellow for medium velocity magnitude.

Figure-4 shows that the distribution of pressure coefficients for different diameters on different positions of the cylinder. Here velocity is fixed for different diameter. The pressure co-efficient is positive at the stagnation point and decreases with the increase of angular position from the forward stagnation point. Near the stagnation region the slope of the curves are higher for larger diameters of the cylinder that means the flow separation occurs earlier in case of larger diameter of the cylinder.

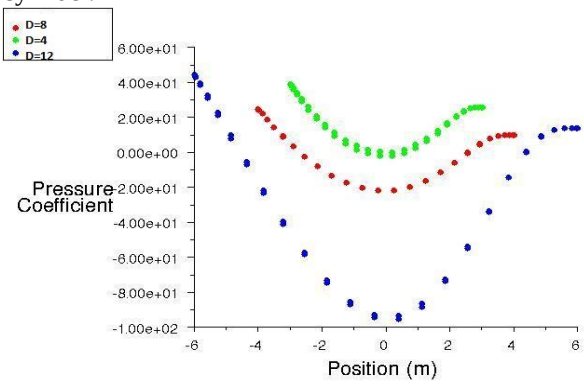

Fig-4: Pressure co-efficient Vs position for different diameter.

From Figure-5 it is seen that skin friction co-efficient increases with the increase of angular position from the forward stagnation point for different diameter of cylinder and at a fixed velocity. After the separation point skin friction co-efficient decreases. At the rear stagnation point shin friction coefficient is lower. At the inflection point skin friction co-efficient is higher.

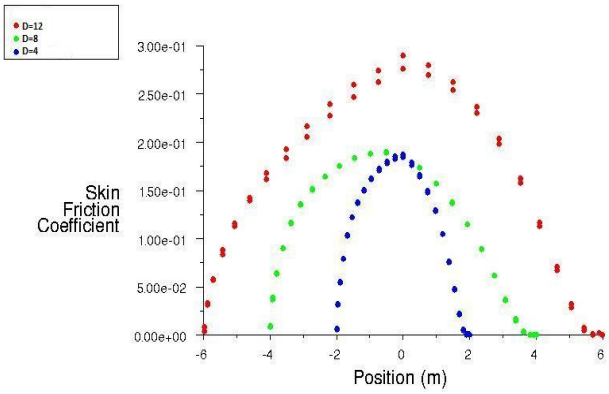

Fig-5: Skin friction co-efficient Vs position for different diameter.

The accuracy of skin friction coefficient prediction in numerical simulations is highly dependent on the accurate resolution of the turbulent boundary layer near the surface of the body. Accurate calculation of near-wall effects requires an extremely fine mesh in that region. Since boundary layer separation arises due to pressure variations, accurate separation point predictions are dependent on accurate pressure calculations, which require a less fine mesh than skin friction calculations.

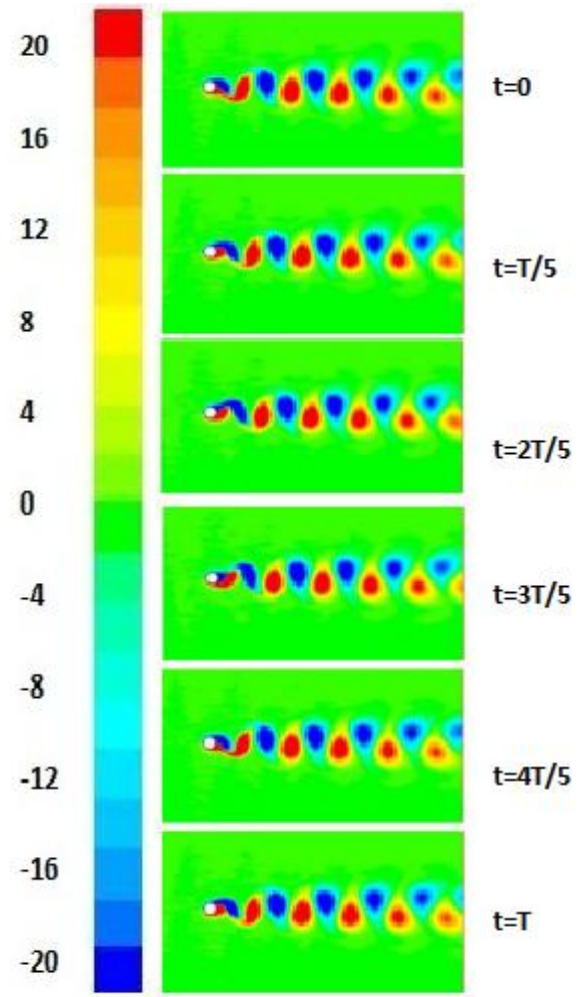

Fig-6: Vorticity magnitude contours.

Vorticity contour plots in Figure 6 shows the motion of the fluid during one vortex shedding cycle. The cycle plotted is between 9.000 and 9.134 seconds of the flow time.The von Karman vortex street is clearly seen on vortices contours.

7. CONCLUSION

The flow around a cylinder in infinite flow has the characteristic tendency of flow separation along with coanda effect making the flow adhere to the surface and delaying the flow separation. The adverse pressure gradient and coanda effect depend upon the magnitude of turbulence intensity and magnitude of approach velocity. For fully developed turbulent velocity profile at approach, the flow adheres to the cylinder due to the coanda effect. These features have significant influence on skin friction and pressure distribution.

The optimum performance of fluid machinery, such as fans, turbines, pumps, compressors, hydrodynamic loading on marine pipelines, risers, offshore platform support legs, chemical mixing, lift enhancement etc. can only be predicted with accurate understanding of flow of separation. By experimental study we have to face lots of problem to find separation point. Computational Fluid Mechanics has become popular to find separation point as well as any simulation of Fluid Mechanics.

8. REFERENCES

[1] Ong, M. C., Utnes, T., Holmedal, L.E., Myrhaug, D., Pettersen, B., "Numerical Simulation of Flow around a Smooth Circular Cylinder at very High Reynolds Numbers", Journal of Marine Structures, vol. 22(2), pp.142-153, 2009.

[2] Gillies, E. A.," Low Dimensional Control of the Circular Cylinder Wake", Journal of Fluid Mechanics, vol. 371, pp. 157-178, doi:10.1017/S0022112098002122, 1998.

[3] Norberg, C., Effects of Reynolds Number and a Low-Intensity Free Stream Turbulence on the Flow around a Circular Cylinder, Chalmers University of Technology, ISSN 02809265, 1987.

[4] Wissink, J. G. and Rodi, W., "Numerical Study of the Near Wake of a Circular Cylinder", International Journal of Heat and Fluid Flow, vol. 29, pp. 1060-1070, 2008.

[5] Travin, A., Shur, M., Strelets, M., Spalart, P., "Detached-Eddy Simulations Past a Circular Cylinder Flow", Turbulence and Combustion, vol. 63, pp. 293- 313, 1999.

[6] E. Achenbach, Journal of Fluid Mechanics, 54 (3), 565 (1972). doi:10.1017/S0022112072000874

[7] Lim, H., Lee, S., "Flow Control of Circular cylinder with Longitudinal Grooved Surfaces", American Institute of Aeronautics and Astronautics Journal, vol. 40(10), pp. 2027-2036, 2002.

[8] Roy, C. J., DeChant, L. J., Payne, J. L. and Blottner,F. G. "Bluff- Body Flow Simulations using Hybrid RANS/LES", American institute of Aeronautics and Astronautics Journal, AIAA 2003-3889, 2003.